

**Quantized phonon modes in loaded polymer films**

David J. Farmer, Andrey V. Akimov, James S. Sharp, and Anthony J. Kent

Citation: *Journal of Applied Physics* **113**, 033516 (2013); doi: 10.1063/1.4774689

View online: <http://dx.doi.org/10.1063/1.4774689>

View Table of Contents: <http://scitation.aip.org/content/aip/journal/jap/113/3?ver=pdfcov>

Published by the [AIP Publishing](#)

---



**Goodfellow**

metals • ceramics • polymers  
composites • compounds • glasses

**Save 5% • Buy online**  
70,000 products • Fast shipping

## Quantized phonon modes in loaded polymer films

David J. Farmer,<sup>1,2</sup> Andrey V. Akimov,<sup>1</sup> James S. Sharp,<sup>1,2</sup> and Anthony J. Kent<sup>1</sup>

<sup>1</sup>*School of Physics and Astronomy, The University of Nottingham, University Park, Nottingham NG7 2RD, United Kingdom*

<sup>2</sup>*Nottingham Nanotechnology and Nanoscience Centre, The University of Nottingham, Nottingham NG7 2RD, United Kingdom*

(Received 2 November 2012; accepted 18 December 2012; published online 18 January 2013)

We study the spectrum of quantized hypersonic vibrations in gold coated polymer films deposited on crystalline silicon substrates. Gold films with thickness values in the range 2.5 nm to 30 nm were deposited onto supported polystyrene films and shifts in the resonant frequency of coated areas were observed relative to the bare polymer films. The experimental results and analysis based on solving the elastic equation with various boundary conditions show that supported polymer films have a potential for application in mass sensing and studies of the nanomechanical response of ultrathin adsorbed layers of material. © 2013 American Institute of Physics.

[<http://dx.doi.org/10.1063/1.4774689>]

### I. INTRODUCTION

The development of gigahertz (GHz) and terahertz (THz) acoustic devices is a challenging task which promises new and attractive applications.<sup>1</sup> A wide class of potential acoustic devices is based on nanostructures where the acoustic phonon spectrum is quantized. Typical examples of such nanostructures are nanomechanical cantilevers, beams, strings, and free standing membranes, where the frequency of quantized phonons detected experimentally reaches hundreds of GHz.<sup>2,3</sup> The most promising applications for devices utilizing quantized phonons are nanosensing,<sup>4,5</sup> optical cooling,<sup>6,7</sup> phonon lasing,<sup>8</sup> and quantum information processing.<sup>9</sup>

The nanostructures used in these previous experiments were usually fabricated from crystalline materials (e.g., silicon). Soft materials, such as polymers, are used more rarely because of the comparatively higher phonon damping that occurs in these materials.<sup>10</sup> Recent experiments, however, with thin polymer films and multilayers have shown that phonon quantization is still very pronounced for frequencies up to a few tens of GHz.<sup>11</sup> In this respect, polymeric nanostructures have a number of advantages when compared with crystalline materials. They do not need to be free-standing and can be supported by solid substrates; phonon quantization is still likely to occur because of the large acoustic mismatch that exists between the polymer and the substrate. Polymers can be routinely fabricated with nanometer dimensions using techniques such as spin-coating or melt processing and additional further patterning of polymer surfaces is also possible using nano-imprint lithography based approaches.<sup>12</sup> Furthermore, block copolymer materials provide a rich variety of architectures that can facilitate the self-assembly of interesting nanostructures with well-defined shapes and sizes.<sup>13</sup> Ultra-thin polymer films have relatively low mass, which could be comparable to the masses of adsorbed materials, making them potentially useful for mass sensors. There is also potential for polymer nanostructures to be integrated with crystalline opto-mechanical and electro-

mechanical devices to provide controlled coupling of phonons and photons (e.g., combined photonic and phononic crystals).

The aim of the present work is to demonstrate the changes to the hypersonic quantized phonon spectrum when a polymer film is loaded with a mass of another material. These experiments are an important demonstration of the potential for using ultra-thin polymer films as mechanical resonators for hypersonic nanosensing applications. We show that, as well as being able to detect adsorbed mass, the polymer films have the potential to provide information about changes in the elastic and mechanical properties of the adsorbed material under certain conditions. Specifically, we analyze the results using two models: the first considers simply loading the polymer film with some mass; and the second includes the elastic coupling of the adsorbed material with the polymer film.

### II. EXPERIMENT

Aluminium (Al) films with a thickness of 75 nm were deposited on the surface of 50  $\mu\text{m}$  thick single crystal silicon (Si) substrates via thermal evaporation. Polystyrene (PS) (Sigma Aldrich,  $M_w = 192$  kDa) films were then spin coated from 2%wt. solutions in toluene on to the reverse side of the Si substrates. A drop of solution was placed on each substrate and rotated at 2000 rpm. This procedure resulted in the production of uniform polymer films with thickness values of  $106 \pm 4$  nm. The thickness of each film was measured using a single wavelength self-nulling ellipsometer (wavelength  $\lambda = 633$  nm). Finally, high purity gold (Au) layers with areas of  $3 \times 2$  mm<sup>2</sup> were deposited on the PS coated surface of the samples using thermal evaporation at a pressure of  $1 \times 10^{-5}$  Torr. The thickness of the Au layers was measured using a quartz crystal resonator that was placed close to the samples in the evaporation chamber. Gold layer thickness values in the range  $2.5\text{--}30 \pm 0.5$  nm were obtained.

The hypersonic experiments were performed at room temperature using a picosecond acoustic technique<sup>14</sup> as

shown in the scheme in Fig. 1. The Al film was excited by 60 fs optical (pump) pulses from an amplified Ti-sapphire laser ( $\lambda = 800$  nm), with a repetition rate of 5 kHz. The pump beam was focused to a  $200 \mu\text{m}$  diameter spot which resulted in the maximum energy density on the Al film being  $\sim 10$  mJ/cm<sup>2</sup>. When the Al film is optically excited in this way it expands thermo-elastically and a bipolar strain pulse with a duration of  $\sim 10$  ps and an amplitude of  $\sim 10^{-3}$  is injected into the neighbouring Si substrate.<sup>14</sup> The strain pulse propagates through the Si with the velocity of longitudinal (LA) sound ( $8430 \text{ ms}^{-1}$ ) and reaches the Si/PS interface in a time of  $\sim 6$  ns. The strain pulse is then partially reflected due to the acoustic mismatch between PS and Si and partially transmitted into the polymer film. This results in a hypersonic wavepacket of coherent LA phonons being excited in the PS film.

The change in the intensity,  $\Delta I(t)$ , of an optical probe pulse ( $\lambda = 400$  nm), originating from the same laser and reflected off the surface of the sample (see Fig. 1), was measured as a function of its delay,  $t$ , relative to the pump pulse. This was achieved using a balanced photodiode and a lock-in amplifier, triggered with a repetition rate of 2.5 kHz using a mechanical chopper locked to the 5 kHz pump beam frequency. For each Au thickness, 5 measurements were taken, each at a different point on the gold coated areas. The measurement positions were chosen to be away from the edges of the gold coated regions so as to avoid any edge effects. The results presented below are the average of these measurements with associated error bars.

The measured temporal signals,  $\Delta I(t)$ , are shown in Fig. 2(a) for various thickness values of the Au load. The changes in the reflectance of the sample start at  $t=0$ , which corresponds to the arrival of the strain pulse at the free surface of the sample (Au/air interface). The signals have a complicated oscillatory behavior which is reproducible at all points on the surface for both the plain PS film and each Au load layer. No significant differences were observed in the shapes of these temporal signals when the excitation pump and probe beam power densities were varied. General features, such as the period of the oscillations, the net decay time, and the amplitude of  $\Delta I(t)$  in the plain (unloaded) PS film (see the upper curve in Fig. 2(a)), were similar to those detected

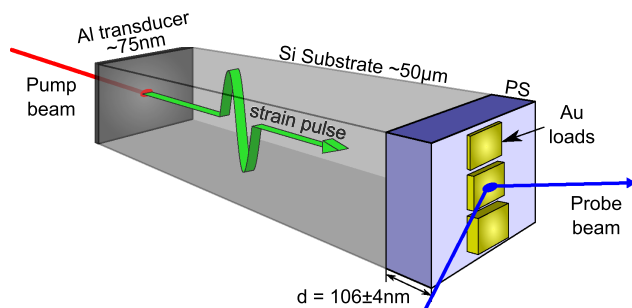


FIG. 1. A schematic diagram showing the experimental setup. The pump beam hits the aluminium transducer causing a thermo-elastic expansion that results in a strain pulse being injected into the silicon substrate. This strain pulse propagates through the silicon and into the polystyrene film and load (if present), where it is measured via the change in intensity of a reflected probe beam.

in earlier work on PS films.<sup>11</sup> It can clearly be seen that the signals change significantly when the thickness of the Au load increases. More specifically, for thick Au films the period of the slower oscillations increases and the high-frequency features are more heavily damped.

Figure 2(b) shows fast Fourier transforms (FFT), obtained in 2 ns time windows, of the corresponding  $\Delta I(t)$  data shown in Fig. 2(a). Two distinct resonant peaks, marked by solid arrows, can easily be seen in the spectra. These peaks correspond to the quantized LA phonon modes in the PS film loaded with Au. The large acoustic mismatch between the PS and Si substrate means that the excited acoustic modes (i.e., phonons) cannot escape easily from the film. In unloaded PS films, such confinement results in quantization that has an analog with closed-pipe organ modes with frequencies of

$$f_n = \frac{(2n+1)s}{4d}, \quad (1)$$

where  $n$  is an integer;  $s$  is the longitudinal (LA) speed of sound in the polymer; and  $d$  is the thickness of the polymer film.<sup>11</sup> The two peaks in the spectrum for the plain (unloaded) PS film [upper curve in Fig. 2(b)] correspond to the modes with frequencies  $f_0$  and  $f_1$  related to  $n=0$  and  $n=1$ , respectively, given by Eq. (1). For Au loaded PS films, Eq. (1) is no longer valid, and the values of  $f_n$  change: the peak frequencies decrease with the increase of the Au load thickness. The magnitude of the changes in  $f_0$  and  $f_1$  following the deposition of Au layers lies in the GHz frequency range and for the highest load (30 nm Au film),  $f_0$  decreases by a factor of 3.

Figure 3 shows how the frequencies,  $f_0$  and  $f_1$ , depend upon the thickness and areal mass density,  $\sigma_{load}$ , of the adsorbed gold layers (lower and upper scales, respectively). These plots show that large relative changes in  $f_0$  and  $f_1$  take place when the Au is only a few nanometers thick. Further increases in thickness up to 30 nm have a tendency to cause saturation of the frequency shifts.

### III. ANALYSIS AND DISCUSSION

The aim of the analysis is to calculate frequencies for quantized LA phonons in the polymer/load structure. This is performed by considering elastic standing waves described by the displacement,  $u(x,t)$ , of atoms in the structure in the direction  $x$ , perpendicular to the surface. The elastic equation for  $u(x,t)$  may be written in the form

$$\rho_m \frac{d^2 u_m(x,t)}{dt^2} - c_{11}^m \frac{d^2 u_m(x,t)}{dx^2} = 0, \quad (2)$$

where  $\rho_m$  and  $c_{11}^m$  are the bulk density and elastic constant of each layer,  $m$ . The potential influence of interfacial effects on the mechanical and acoustic properties of the PS films was considered. Previous work by Kehoe *et al.*<sup>15</sup> studied ultrathin poly(methyl methacrylate) (PMMA) films and concluded that the speed of sound and Young's modulus started to deviate from their bulk values when the film thickness was  $< 80$  nm. Other works report the thickness value where

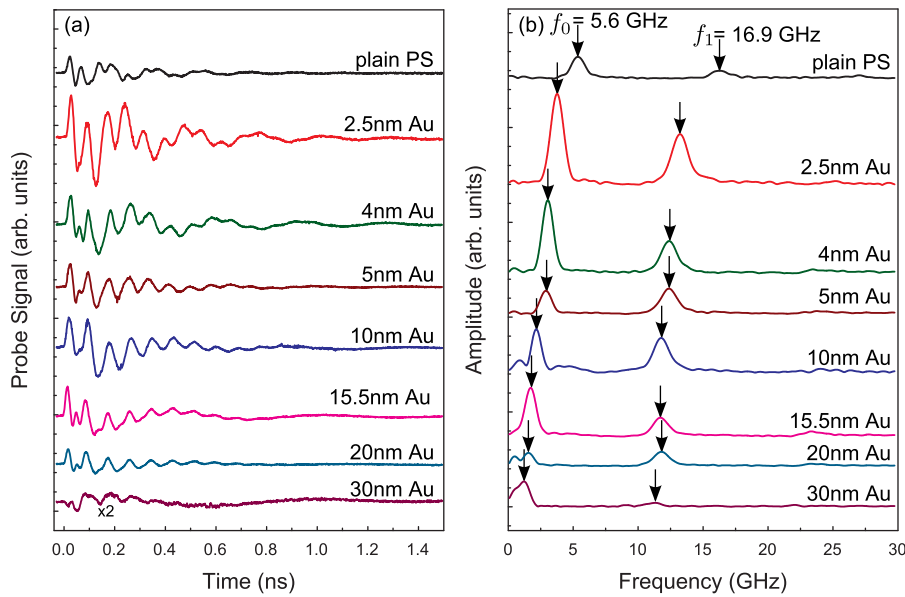


FIG. 2. (a) Representative examples of temporal changes in the reflectivity of the probe beam,  $\Delta I(t)$ , measured using for probing 400 nm, femtosecond laser pulses at the surface of unloaded and Au loaded polystyrene films; (b) amplitude fast Fourier transform spectra obtained from the corresponding temporal traces shown in (a). The vertical arrows indicate the frequencies  $f_0$  and  $f_1$  of the fundamental and first phonon quantized resonances, respectively. The thicknesses of the Au films are indicated above each curve.

these properties change to be  $\sim 40$  nm.<sup>16,17</sup> Both of these thicknesses fall below that of the PS films used in this study so no deviation from the bulk properties is expected. Furthermore, while studies have shown that the properties of PMMA are extremely sensitive to substrate interactions,<sup>18</sup> PS films have been shown to have properties that are insensitive to both substrate interactions and the presence of an evaporated metal layer.<sup>16</sup>

The solution of Eq. (2) gives a discrete spectrum of phonon modes defined by the parameters of the PS film, Au load, and boundary conditions at the interfaces. At the PS/Si interface, we assume that the film is pinned, i.e.,  $u = 0$ , which is a good approximation due to the large acoustic mismatch between PS and Si. At the free surface, the strain is expected to be zero, i.e.,  $du/dx = 0$ . For the PS/Au interface, we con-

sider two separate cases that are described by two different boundary conditions. The first, which we shall call a “load” model, assumes that no elastic waves are excited in the Au load, which has a mass per unit area,  $\sigma_{load}$ . This is equivalent to the assumption that the entire Au load matches the displacements at the PS/Au interface. The boundary condition in this case may be written as

$$c_{11}^{PS} \frac{du_{PS}}{dx} \Big|_{x=d} = \sigma_{load} \frac{d^2 u_{PS}}{dt^2} \Big|_{x=d} \quad (3)$$

and the frequencies  $\omega_n = 2\pi f_n$  of the quantized phonon eigenmodes may be found from the following equation:

$$\tan\left(\frac{\omega d}{s_{PS}}\right) \omega \sigma_{load} = Z_{PS}, \quad (4)$$

where  $Z_{PS} = s_{PS} \rho_{PS}$  is the acoustic impedance of the PS film. The second case, referred to as the “elastic” model, is when the elastic wave extends into the Au load. Then, the boundary condition at  $x = d$  is obtained by matching the displacement and stress in the film and load and we have

$$u_{PS}(d, t) = u_{load}(d, t), \quad (5a)$$

$$c_{11}^{PS} \frac{du_{PS}}{dx} \Big|_{x=d} = c_{11}^{load} \frac{du_{load}}{dx} \Big|_{x=d} \quad (5b)$$

and we get the spectrum of phonon eigenmodes from the following equation:

$$\tan\left(\frac{\omega d}{s_{PS}}\right) \tan\left(\frac{\omega \sigma_{load}}{Z_{load}}\right) = \frac{Z_{PS}}{Z_{load}}, \quad (6)$$

where  $Z_{load}$  is the acoustic impedance of the Au layer. The calculations using Eqs. (4) and (6) for an Au load have been performed for the following parameters:  $d = 105$  nm,  $s_{PS} = 2300$  m/s,  $s_{Au} = 3200$  m/s,  $\rho_{PS} = 1047$  kg/m<sup>3</sup>, and  $\rho_{Au} = 19\,300$  kg/m<sup>3</sup>. The dependence of  $f_n$  on  $\sigma_{load}$  for  $n = 0$

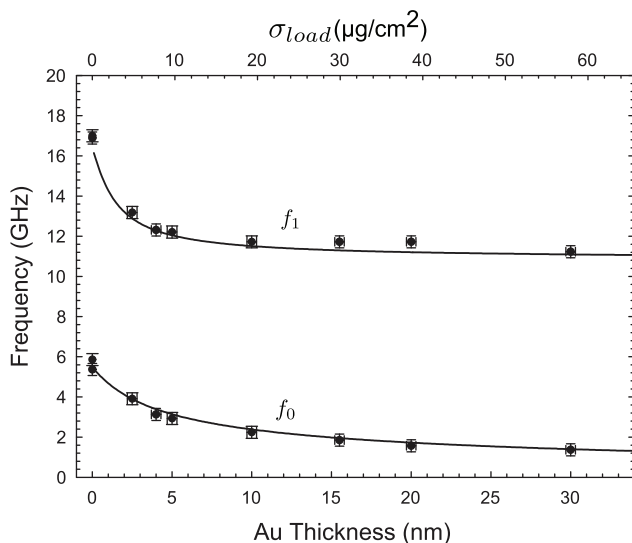


FIG. 3. Measured (symbols) and calculated (solid curves) fundamental and first harmonic quantized phonon frequencies of loaded PS films as a function of the mass (upper scale) and thickness (lower scale) of the deposited Au load. The calculations obtained for the “load” and “elastic” models are the same to within the level of uncertainty.



and  $n = 1$  are shown in Fig. 3 as solid lines. The results of the calculations for the two models are almost identical and indistinguishable in Fig. 3. Both the load and elastic models fit the experimental results very well.

The appearance of a strong non-linearity of the frequency dependence on the areal mass density of the applied load is to be expected already on a qualitative level and occurs at load thickness values of  $d \sim 1$  nm ( $\sigma_{load} \approx 2 \mu\text{g}/\text{cm}^2$ ). An obvious explanation for this is that in our experiment the ratio of areal densities  $\sigma_{load}/\sigma_{PS}$  is not a negligibly small value. If the deposited load is small, then it couples to the oscillations of the resonator and, analogous to the Sauerbrey equation that is commonly used to calculate the sensitivity of quartz crystal microbalance (QCM) systems,<sup>19</sup> can be assumed to act like a small increase in the mass, or thickness, of the film. The corresponding change in frequency, as described by Eq. (1), allows the ultimate frequency sensitivity of the polymer film to deposited mass to be estimated. For the structure presented here ( $d = 105$  nm,  $s_{PS} = 2300$  m/s), a sensitivity of  $650 \text{ ag}/(\text{cm}^2 \text{ Hz})$  is obtained.

In the general case, where the mass of the load becomes comparable to the mass of the oscillator, the change in resonant frequency must be obtained by Eq. (4) or Eq. (6). It is useful to find the conditions under which the load and elastic models give essentially different eigenmode frequencies for quantized phonons. For this, we have performed calculations for a wide range of load parameters,  $\sigma_{load}$  and  $Z_{load}$ . Figure 4(a) shows the dependence of the  $n = 1$  quantized frequency,  $f_1$ , on the mass of the load relative to our PS film. The solid curve is the calculated result of the load model [Eq. (4)] and dashed curves are calculated using the elastic model [Eq. (6)] for two values of load impedance. It is seen that the load model is valid only for low  $\sigma_{load}$ . The difference in the results for two models also becomes larger as  $Z_{load}$  decreases. Figure 4(b) shows a surface plot where the difference between the first quantized frequencies,  $\delta f$ , calculated using each model is plotted as a function of  $\sigma_{load}$  and  $Z_{load}$ . In the regions where  $\delta f/\Delta f \approx 0$ , both models give almost identical results. There are, however, a wide range of  $\sigma_{load}$  and  $Z_{load}$  values where a thin PS film is very sensitive to the elastic properties of the load, as well as its mass.

A practical question arises regarding the validity of the load or elastic model in each particular case. From Fig. 4, it is clear that these two models give identical results when

$\sigma_{load}$  is negligible relative to the mass of the sensor for any  $Z_{load}$ . This is commonly the situation that occurs when using commercial QCMs, as the quartz crystals are relatively large. For low mass sensors, such as the  $\sim 100$  nm polymer film used in the present experiment the ratio  $\sigma_{load}/\sigma_{PS}$  is not negligible. For even the smallest (2.5 nm) Au film studied here,  $\sigma_{load}/\sigma_{PS} = 0.5$ . When probing, for example, various organic materials, this ratio will be less (although still far from zero) and the question regarding the validity of the load or elastic model in each case becomes increasingly important. In reality, the answer depends on whether the load is in good elastic contact with the polymer film. If the contact is poor then the load model is capable of reproducing the observed frequency shifts. If there is intimate contact between the PS sensor layer and the attached load, then the elastic model becomes more suitable. In the latter case, the results obtained by load and elastic model calculations differ significantly if  $Z_{load}/Z_{PS} < 2$ . For Au loads studied here,  $Z_{load}/Z_{PS} = 26$  and consequently the analysis gives the same frequency shifts using either model.

Our results point to the potential application of polymer films as ultrasensitive-hypersonic sensors for investigating a variety of systems. At low masses ( $< \sim 10 \text{ ng cm}^{-2}$ ), the specific sensitivity to changes in mass deposited on the polymer surface is estimated from Fig. 3 to be about  $650 \text{ ag}/(\text{cm}^2 \text{ Hz})$ . This is approximately 8 orders of magnitude better than current state-of-the-art QCM systems, due to the higher frequency used. However, the actual mass sensitivity that can be achieved in practice is limited by the precision with which changes in the frequency can be measured. This depends both on the damping and the signal to noise ratio. The damping lowers the Q of the system, and hence leads to broadening of the spectral lines, but if the signal to noise ratio is sufficiently high, it is possible to measure the shift of a line which is some fraction of its linewidth. In our experiment, the frequency resolution is  $\sim 100$  MHz, which is about 10% of the linewidth. This corresponds to being able to detect areal mass densities of  $65 \text{ ng}/\text{cm}^2$ , which is only one order of magnitude worse than state-of-the-art QCM systems that can resolve a fraction of a Hz at about 10 MHz. It is possible that the frequency resolution of the experiments reported here could be improved by increasing the signal to noise ratio by, for example, using a higher repetition rate femtosecond oscillator instead of the amplified femtosecond laser (we

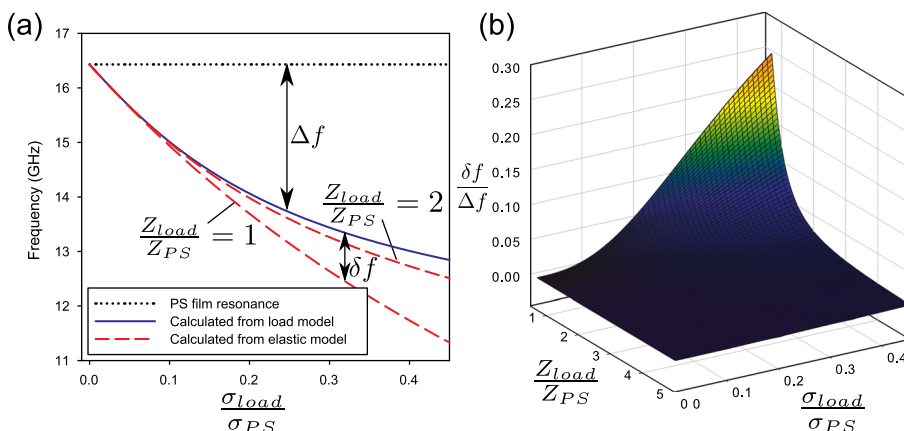


FIG. 4. Results of calculations of the shift in the first harmonic frequency,  $f_1$ , against areal mass density for a 100 nm polystyrene film loaded with material with acoustic impedance  $Z_{load}$ : (a) the solid curve is obtained using the load model and two dashed curves correspond to the elastic model for  $Z_{load} = 1$  and 2; (b) a surface plot of the relative difference in frequency as calculated by the load and elastic models as a function of the relative mass and impedance of the load.

should point out here that the pump beam from the amplified laser was heavily attenuated, and it would be possible to achieve similar pump power density using a femtosecond oscillator if the spot was focused to  $\sim 10\ \mu\text{m}$ ). Given that the mass sensitivities are similar, and the current requirement for an ultrafast laser, it seems unlikely that the polymer based sensor could compete with the, much simpler to operate, QCM sensors except with regard to potentially better spatial resolution to adsorbed mass as the laser spot is small ( $\sim 100\ \mu\text{m}$ ) compared to typical QCM sensors ( $\sim 1\ \text{cm}^2$ ). However, the above comparisons of the polymer device with QCMs assume a vacuum or gas environment. Applications of QCMs in studies of, for example, protein adsorption on surfaces require operation in liquids where strong damping significantly decreases their sensitivity. The advantage of a sensor working at frequencies in the tens of GHz range is that it will be largely mechanically decoupled from fluids with viscosity comparable to water, and so, in this regime the ultimate sensitivity of a polymer hypersonic mass sensor could be better than QCMs. It is also expected that the mass changes and acoustic impedances of organic materials, such as proteins, will lie in the region where the frequency shift is sensitive to  $Z_{load}$ , possibly allowing for additional information regarding the mechanical and elastic properties of the load to be extracted. These potential advantages of the polymer-based device could be more easily exploited with the use of electrical means of generation and detection of acoustic waves in the tens of GHz range.

#### IV. CONCLUSIONS

In conclusion, we have shown that the frequencies of quantized GHz phonon modes in ultra-thin polymer films are sensitive to adsorbed material. The frequency shifts lie in the GHz range and a decrease in frequency of a factor of 3 is detected for the fundamental mode when loading a  $\sim 100\ \text{nm}$  polystyrene film with a 10 nm film of gold. The results are analyzed using models where the polymer film is coupled or alternatively decoupled elastically to/from the load. The

calculations performed suggest that under certain conditions the film is very sensitive not only to the areal mass density of the load but also to its acoustic impedance as well. These results suggest potential applications for the films as ultra-sensitive hypersonic mass sensors.

#### ACKNOWLEDGMENTS

We acknowledge financial support for this work from the UK Engineering and Physical Sciences Research Council (Grant No. EP/H004939/1).

- <sup>1</sup>T. Gorishnyy, M. Maldovan, C. Ullal, and E. L. Thomas, *Phys. World* **18**, 24 (2005).
- <sup>2</sup>M. Poot and H. S. J. van der Zant, *Phys. Rep.* **511**, 273 (2012).
- <sup>3</sup>A. Bruchhausen, R. Gebbs, F. Hudert, D. Issenmann, G. Klatt, A. Bartels, O. Schecker, R. Waitz, A. Erbe, E. Scheer, J. Huntzinger, A. Mlayah, and T. Dekorsy, *Phys. Rev. Lett.* **106**, 077401 (2011).
- <sup>4</sup>K. Jensen, K. Kim, and A. Zettl, *Nat. Nanotechnol.* **3**, 533 (2008).
- <sup>5</sup>Y. T. Yang, C. Callegari, X. L. Feng, K. L. Ekinci, and M. L. Roukes, *Nano Lett.* **6**, 583 (2006).
- <sup>6</sup>J. Chan, T. P. M. Alegre, A. H. Safavi-Naeini, J. T. Hill, A. Krause, S. GroËblacher, M. Aspelmeyer, and O. Painter, *Nature* **478**, 89 (2011).
- <sup>7</sup>J. D. Teufel, T. Donner, D. Li, J. W. Harlow, M. S. Allman, K. Cicak, A. J. Sirois, J. D. Whittaker, K. W. Lehnert, and R. W. Simmonds, *Nature* **475**, 359 (2011).
- <sup>8</sup>I. S. Grudinin, H. Lee, O. Painter, and K. J. Vahala, *Phys. Rev. Lett.* **104**, 083901 (2010).
- <sup>9</sup>A. D. O'Connell, M. Hofheinz, M. Ansmann, R. C. Bialczak, M. Lenander, E. Lucero, M. Neeley, D. Sank, H. Wang, M. Weides, J. Wenner, J. M. Martinis, and A. N. Cleland, *Nature* **464**, 697 (2010).
- <sup>10</sup>C. J. Morath and H. J. Maris, *Phys. Rev. B* **54**, 203 (1996).
- <sup>11</sup>A. V. Akimov, E. S. K. Young, J. S. Sharp, V. Gusev, and A. J. Kent, *Appl. Phys. Lett.* **99**, 021912 (2011).
- <sup>12</sup>S. Y. Chou, P. R. Krauss, and P. J. Renstrom, *Science* **272**, 85 (1996).
- <sup>13</sup>C. Park, J. Yoon, and E. L. Thomas, *Polymer* **44**, 6725 (2003).
- <sup>14</sup>C. Thomsen, H. T. Grah, H. J. Maris, and J. Tauc, *Phys. Rev. B* **34**, 4129 (1986).
- <sup>15</sup>T. Kehoe, J. Bryner, V. Reboud, J. Dual, and C. M. S. Torres, *J. Phys.: Conf. Ser.* **214**, 012049 (2010).
- <sup>16</sup>J. Sharp and J. Forrest, *Phys. Rev. Lett.* **91**, 235701 (2003).
- <sup>17</sup>J. L. Keddie, R. A. L. Jones, and R. A. Cory, *EPL* **27**, 59 (1994).
- <sup>18</sup>J. Sharp and J. Forrest, *Phys. Rev. E* **67**, 031805 (2003).
- <sup>19</sup>G. Sauerbrey, *Z. Phys.* **155**, 206 (1959).